AStA Advances in Statistical Analysis
https://doi.org/10.1007/s10182-024-00499-x

ORIGINAL PAPER

Testing for periodicity at an unknown frequency under cyclic long memory, with applications to respiratory muscle training

Jan Beran[1] · **Jeremy Näscher**[1] · **Fabian Pietsch**[2] · **Stephan Walterspacher**[3,4]

Received: 13 June 2023 / Accepted: 18 March 2024

Abstract
A frequent problem in applied time series analysis is the identification of dominating periodic components. A particularly difficult task is to distinguish deterministic periodic signals from periodic long memory. In this paper, a family of test statistics based on Whittle's Gaussian log-likelihood approximation is proposed. Asymptotic critical regions and bounds for the asymptotic power are derived. In cases where a deterministic periodic signal and periodic long memory share the same frequency, consistency and rates of type II error probabilities depend on the long-memory parameter. Simulations and an application to respiratory muscle training data illustrate the results.

Keywords Cyclic long memory · Periodicity · Deterministic periodicity · Periodogram · Gegenbauer process

1 Introduction

The issue of identifying periodic components is at the core of time series analysis. A particularly strong type of stochastic periodicity is periodic long memory (see Hosking 1981; Anděl 1986; Gray et al. 1989, 1994; Giraitis and Leipus 1995; Woodward et al. 1998). Stationary processes with periodic long memory are characterized by a spectral density function

✉ Jan Beran
jan.beran@uni-konstanz.de

[1] Department of Mathematics and Statistics, University of Konstanz, Konstanz, Germany

[2] Asklepios Klinikum Harburg, Hamburg, Germany

[3] Medical Clinic - Department of Pneumology, Klinikum Konstanz, Konstanz, Germany

[4] Faculty of Health/School of Medicine, Witten/Herdecke University (UW/H), Witten, Germany

Published online: 12 April 2024

$$f(\lambda) \sim c_f \left|\lambda - \omega_0\right|^{-2d} \ (\lambda \to \omega_0) \tag{1}$$

where $0 < \omega_0 < \pi$, $0 < c_f < \infty$ and $d \in (0, \frac{1}{2})$. Here, "$\sim$" means that the ratio of the left and right hand side converges to one. Typical examples are GARMA processes introduced in Anděl (1986) and Gray et al. (1989, 1994) (also see Hosking 1981). For instance, the simplest GARMA process, also called Gegenbauer process, is defined by

$$\left(1 - 2\cos\omega_{0,X} B + B^2\right)^d X_t = \varepsilon_t \tag{2}$$

where B is the backshift operator and ε_t are iid zero mean random variables with $\sigma_\varepsilon^2 = var(\varepsilon_t) < \infty$ (Gray et al. 1989). A natural question that arises is, to what extent is it possible to distinguish periodic long memory from deterministic periodicity. Thus, consider a time series of the form $Y_t = \mu + S_t + X_t$ where S_t is a deterministic periodic function with period $T_{0,S} = 2\pi/\omega_{0,S}$ for some $\omega_{0,S} \in (0, \pi)$, and X_t is a zero mean stationary process with spectral density f such that (1) holds for some $\omega_0 = \omega_{0,X} \in (0, \pi)$. In this paper, a simple class of tests is proposed for $H_0 : S_t \equiv 0$ against the alternative that S_t is not identically equal to zero. Technically, Y_t will be assumed to be a superposition of a harmonic process S_t and a purely stochastic process X_t. The proposed test statistics are motivated by a discrete Whittle approximation of a Gaussian log-likelihood function. Asymptotic rejection regions and bounds for rates at which the probability of the type II error converges to zero are derived. As expected, the most difficult case occurs when $\omega_{0,S} = \omega_{0,X}$, because a jump in the spectral distribution F_X may have a similar finite sample effect on the periodogram as periodic long memory. Asymptotically, this results in a slower decay of the type II error probability. Typical data examples are displayed in Figs. 1 and 2. The time series in Figs. 1a and 2a represent the breathing effort of the diaphragm during two types of respiratory training. For more detailed explanations see Sect. 5.2 below. Visually, it seems quite difficult to tell in how far peaks in the two periodograms (Figs. 1c and 2c) correspond to deterministic or stochastic periodicity, or to a mixture of both phenomena. The proposed test statistics help to shed some light on this issue (see Sect. 5.2).

In view of the fact that distinguishing between a jump of F_X and a pole of the spectral density is difficult, one may ask the question in how far the distinction is relevant in practice. The fundamental difference is predictability. Consider for instance the optimal linear forecast $\hat{X}_{t+1}$ of X_{t+1} given X_s ($s \le t$), which minimizes the mean squared prediction error $MSE = E[(\hat{X}_{t+1} - X_{t+1})^2]$. Suppose first that $dF_X(\lambda) = 0$ $(\lambda \neq \pm\omega_{0,S})$ and $dF_X(\pm\omega_{0,S}) > 0$ for some $\omega_{0,S} \in (0, \pi)$. Then the process is deterministic and perfect linear prediction possible, i.e. $MSE = 0$. On the other hand, suppose that the spectral density $f_X = F_X'$ of X_t exists everywhere, is continuous for $\lambda \neq \pm\omega_0$, $f(\lambda) > 0$ everywhere and $f_Y(\lambda) \sim c_f|\lambda - \omega_0|^{-2d}$ $(\lambda \to \pm\omega_0)$ for some $d \in (0, \frac{1}{2})$, $0 < c_f < \infty$. Then, in contrast to the first case, X_t is purely stochastic and perfect prediction is not possible, i.e. $MSE > 0$. Similar remarks apply to more general processes, and other questions of statistical

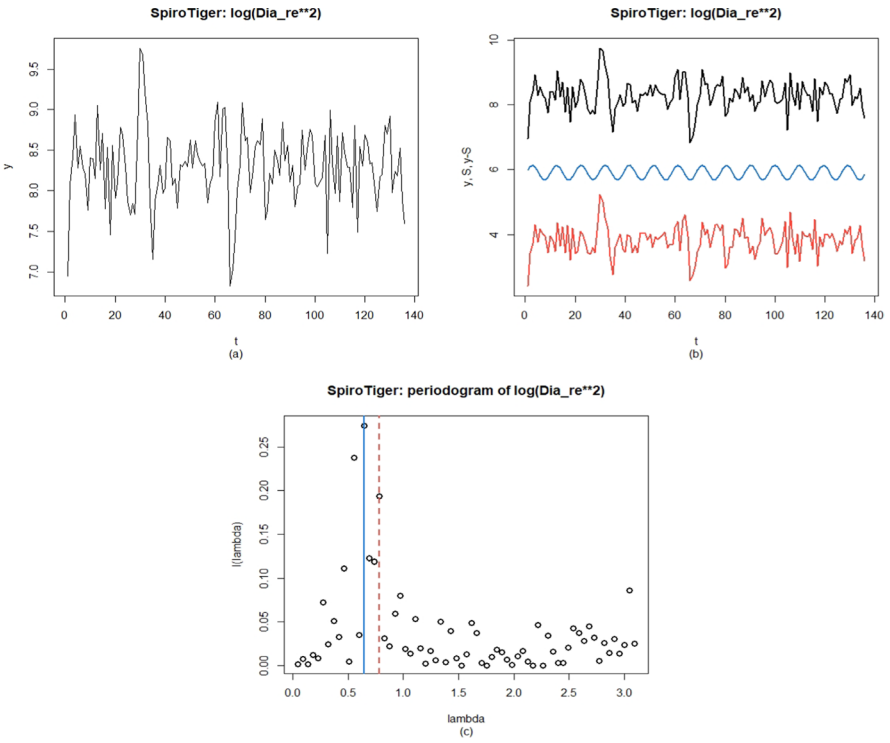

Fig. 1 Measurements of muscular effort of the diaphragm during a *SpiroTiger* exercise. **a** and **b** show the observed series Y_t. In **b**, S_t and $Y_t - S_t$ are also displayed, shifted vertically for better visibility. The periodogram is shown in **c**. (The notation "Dia_re" stands for "diaphragm, right electrode")

inference, in particular if the main focus is on cyclic features of the data generating process.

The introduction of second order stationary processes with poles of the spectral density at non-zero frequencies (Anděl 1986; Gray et al. 1989; Giraitis and Leipus 1995; Woodward et al. 1998) lead to an extended literature in the following decades. Arteche and Robinson (2000), Hidalgo and Soulier (2004), Hidalgo (2005), Hsu and Tsai (2009), Alomari et al. (2020), Arteche (2020), Ayache et al. (2022) and Beaumont and Smallwood (2022) consider semiparametric inference in cyclical long memory processes. Gray et al. (1989), Chung (1996a, 1996b), Woodward et al. (1998), Giraitis et al. (2001), Palma and Chan (2005), Dissanayake et al. (2016) discuss parametric estimation. For model selection see e.g. Leschinski and Sibbertsen (2019). For economic time series see e.g. Porter-Hudak (1990), Ray (1993), Ramachandran and Beaumont (2001), Bisaglia et al. (2003), Caporale and Gil-Alana (2011, 2014), and Gil-Alana et al. (2015). Other areas of application include climatology (Lustig et al. 2017), hydrology (Montanari et al. 2000), traffic modelling (Diongue and Ndongo 2016) and environmental research (Reisen et al. 2014). For further literature see e.g. Hassler

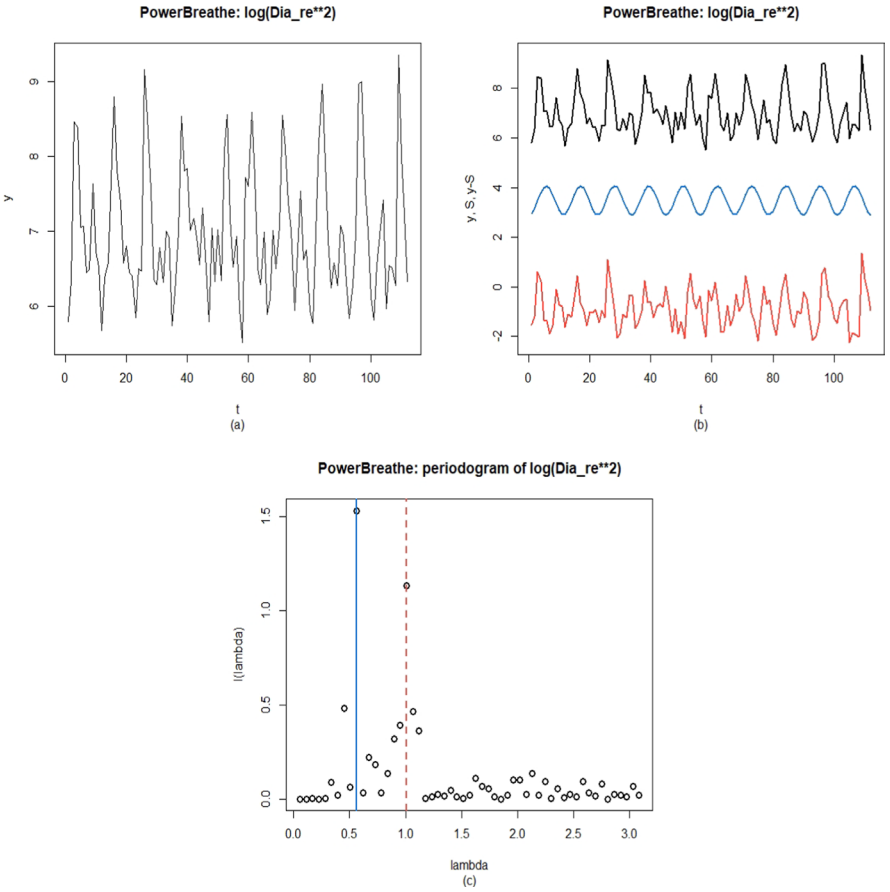

Fig. 2 Measurements of muscular effort of the diaphragm during a *POWERbreathe* exercise. **a** and **b** show the observed series Y_t. In **b**, S_t and $Y_t - S_t$ are also displayed, shifted vertically for better visibility. The periodogram is shown in **c**

(1994), Lapsa (1997), Ferrara and Guégan (2001), Whitcher (2004), Hidalgo (2007), Olenko (2013), McElroy and Holan (2012), Espejo et al. (2015), Hunt et al. (2022) and references therein. An excellent review is given in Dissanayake et al. (2018). An overview of the literature on long-memory processes can be found for instance in Beran et al. (2013) and Pipiras and Taqqu (2017).

The paper is organized as follows. Basic definitions and assumptions are given in Sect. 2. Test statistics are defined in Sect. 3. Asymptotic rejection regions are obtained, and the asymptotic behaviour of type II error probabilities is investigated, under the assumption that model parameters are known. The case of unknown model parameters is considered in Sect. 4. The methods are illustrated by a simulation study and a data example in Sect. 5. Final remarks in Sect. 6 conclude the paper. Proofs, tables and figures are given in the "Appendix".

2 Definitions and preliminary results

Without loss of generality, we may assume $\mu = 0$, i.e. $Y_t = S_t + X_t$. More specifically, the following assumptions will be used:

- (A1)

$$Y_t = S_t + X_t \ (t \in \mathbb{Z}) \tag{3}$$

where X_t and S_t are two independent zero mean second order stationary processes with spectral representations

$$X_t = \int_{-\pi}^{\pi} \exp(it\lambda) dZ_X, \ S_t = \int_{-\pi}^{\pi} \exp(it\lambda) dZ_S, \tag{4}$$

autocovariance functions

$$\gamma_X(k) = \int_{-\pi}^{\pi} \exp(ik\lambda) dF_X(\lambda), \ \gamma_S(k) = \int_{-\pi}^{\pi} \exp(ik\lambda) dF_S(\lambda). \tag{5}$$

Moreover, $F_X' = f_X$ exists everywhere and

$$dF_S(\lambda) = 0 \ (\lambda \neq \pm\omega_{0,S}), \ dF_S(\lambda) = \sigma_S^2 \geq 0 \ (\lambda = \pm\omega_{0,S}) \tag{6}$$

for some $\omega_{0,S} \in (0, \pi)$, $0 \leq \sigma_S^2 < \infty$.

- (A2)

$$X_t = \sum_{j=0}^{\infty} b_j \varepsilon_{t-j} \tag{7}$$

where ε_t $(t \in \mathbb{Z})$ are iid random variables with $E(\varepsilon_t) = 0$ and $\sigma_\varepsilon^2 = var(\varepsilon_t) < \infty$, and the coefficients b_j are such that

$$b_j = j^{d-1}\left(c_b \cos\left(j\omega_{0,X}\right) + o(1)\right) \ (j \to \infty) \tag{8}$$

for some $0 < d < \frac{1}{2}$, $\omega_{0,X} \in (0, \pi)$, $0 < c_b < \infty$.

- (A3) There is an $\eta > 0$ such that

$$E\left(\left|\varepsilon_t\right|^{4+\eta}\right) < \infty.$$

- (A4) Let

$$\tilde{b}(\lambda) = \sum_{j=0}^{\infty} b_j e^{ij\lambda} \ (\lambda \in [0, \pi]).$$

Then, uniformly in $\lambda \in [0, \pi] \setminus \{\omega_{0,X}\}$,

$$\left|\frac{d}{d\lambda}\tilde{b}(\lambda)\right| = O\Big(\big|\tilde{b}(\lambda)\big|\big|\lambda-\omega_{0,X}\big|^{-1}\Big).$$

- (A5) Let Θ_τ be an open subset of $\mathbb{R}^p$, $\Theta_d = (0, \frac{1}{2})$, $\Psi_{\sigma^2} = \mathbb{R}_+$, $\Psi_\omega = (0, \pi)$, $\Theta = \Theta_d \times \Theta_\tau$ and $\Psi = \Psi_{\sigma^2} \times \Psi_\omega \times \Theta$. For $p = 0$, we set $\Theta_\tau = \varnothing$. Also, let L be an even function of λ such that $0 < c < |L(\lambda;\tau)| < \infty$ for some constant c, and all first and second partial derivatives of L with respect to (λ, τ) are continuous. We denote by $\mathcal{F}_f = \{f(\lambda;\psi), \psi \in \Psi\}$ a parametric family of spectral densities

$$f(\lambda;\psi) = f_X\big(\lambda;\sigma_\varepsilon^2,\omega,d,\tau\big) = \frac{\sigma_\varepsilon^2}{2\pi}g(\lambda;\omega,d,\tau)\ (\lambda\in[-\pi,\pi])$$

where

$$g(\lambda;\omega,\theta) = \left|4\sin\left(\frac{\lambda+\omega}{2}\right)\sin\left(\frac{\lambda-\omega}{2}\right)\right|^{-2d}|L(\lambda;\tau)|^2, \tag{9}$$

$$\int_{-\pi}^{\pi}\log g(\lambda;\omega,\theta)d\lambda = 0,$$

and $\psi = (\sigma_\varepsilon^2,\omega,\theta) = (\sigma_\varepsilon^2,\omega,d,\tau) \in \Psi$. The process X_t is assumed to have a spectral density $f\big(\lambda;\psi_X^0\big) \in \mathcal{F}_f$ with $\psi_X^0 = (\sigma_0^2,\omega_{0,X},d_0,\tau_0) \in \Psi$.
- (A6)

$$\inf_{\omega\in\Psi_\omega,d\in\Theta_d,\tau\in\Theta_\tau}\int_{-\pi}^{\pi}\frac{g\big(\lambda;\omega_{0,X},d_0,\tau_0\big)}{g(\lambda;\omega,d,\tau)}d\lambda = 2\pi.$$

- (A7) For $(\omega,\theta) \in \Psi_\omega \times \Theta$, denote by $\Lambda_0(\omega,\theta) \subset [0,\pi]$ the set of all frequencies λ such that $g(\lambda;\omega,\theta) \neq g\big(\lambda;\omega_{0,X},\theta_0\big)$. Then $(\omega,\theta) \neq (\omega_{0,X},\theta_0)$ implies that $\Lambda_0(\omega,\theta)$ has positive Lebeque measure.
- (A8) Let

$$W(\omega,\theta) = \frac{1}{4\pi}\int_{-\pi}^{\pi}\frac{\partial}{\partial\theta}\log g(\lambda;\omega,\theta)\Big(\frac{\partial}{\partial\theta}\log g(\lambda;\omega,\theta)\Big)^T d\lambda.$$

Then $W(\omega_{0,X},\theta_0)$ is positive definite.

Assuming that X_t has cyclic long memory as defined in (A5), we are interested in testing

$$H_0 : \sigma_S^2 = 0 \text{ versus } H_1 : \sigma_S^2 > 0. \tag{10}$$

Under H_0, $Y_t = X_t$ is a stationary linear processes with cyclic long memory, characterized by the parameter vector $\psi_X^0 = (\sigma_0^2,\omega_{0,X},d_0,\tau_0)$. Estimation of ψ_0 has been studied by various authors (see e.g. Gray et al. 1989; Chung 1996a, b; Woodward et al. 1998; Giraitis et al. 2001). For instance, Giraitis et al. (2001) considered Whittle estimation of θ_0 and $\omega_{0,X}$. The Whittle estimator $(\hat{\omega}_{0,X;\text{Whittle}},\hat{\theta}_{0;\text{Whittle}})$ is defined by minimizing

$$Q_{n,X}(\omega,\theta)=\frac{1}{n}\sum_{j=1}^{m}\frac{I_{X,n}(\lambda_j)}{g(\lambda_j;\omega,\theta)} \tag{11}$$

with respect to (ω,θ). Here, we use the notation $m=[n/2]$ and $\lambda_j=2\pi j/n$ $(j=1,...,m)$. Under assumptions (A2) to (A8), Giraitis et al. (2001) derived consistency of the form $\hat{\theta}_{\text{Whittle}}-\theta_0=O_p(n^{-\frac{1}{2}})$ and $\hat{\omega}_{0,X;\text{Whittle}}-\omega_{0,X}=O_p(n^{-1})$, as well as asymptotic normality of $\sqrt{n}(\hat{\theta}_{\text{Whittle}}-\theta_0)$. They also conjectured that, in spite of n^{-1}–consistency, no asymptotic distribution exists for $\hat{\omega}_{0,X;\text{Whittle}}$. In view of the asymptotic results in Giraitis et al. (2001), a natural statistic for testing (10) is given by

$$T_n=T_n(\psi_X^0)=n^{-\frac{1}{2}}\sum_{\substack{j=1\\ \lambda_j\neq\omega_{0,X}}}^{m}\left(\frac{I(\lambda_j)}{f(\lambda_j;\psi_X^0)}-1\right). \tag{12}$$

Remark 1 Let $0<\lambda<\pi$. Then, under H_0, the expected value of $I(\lambda)$ is asymptotically equal to $f(\lambda;\psi_X^0)$. Therefore, $E[I(\lambda)/f(\lambda;\psi_X^0)]-1=0$. On the other hand, consider the alternative with $dF_S(\lambda)>0$ $(\lambda=\omega_{0,S}\in(0,\pi))$. Then, for λ in the neighborhood of $\omega_{0,S}$, the periodogram of S_t tends to infinity at the rate n. Therefore, the statistic T_n is expected to be large under H_1. It is shown in the next section that T_n indeed tends to infinity in probability.

Remark 2 Condition (8) in assumption (A2) is needed to obtain a pole of the spectral density at $\omega_0=\omega_{0,S}$ as defined in (1) and (9). Assumptions (A3) to (A8) are adopted from Giraitis et al. (2001). These are technical assumptions needed for obtaining asymptotic normality of T_n und H_0. Specifically, the moment assumption (A3) is needed because the periodogram is based on sample autocovariances; (A4) is needed for approximating the spectral density near its pole; (A5) specifies the parametrization; (A6), (A7) are related to identifiability of parameters; (A8) is needed to avoid a degenerate asymptotic distribution.

3 Testing with known parameters

First we consider the case where $\omega_{0,S}$, $\omega_{0,X}$ and θ are known. We will use the notation "$\to_d$" for convergence in distribution, and "$\to_p$" for convergence in probability. Under H_0, T_n has the following asymptotic distribution.

Theorem 1 *Suppose that* (A1) *to* (A8) *hold. Denote by* κ_4 *the kurtosis of* ε_t. *Then, under* H_0,

$$T_n\underset{d}{\to}\sigma_T Z \tag{13}$$

where Z is a standard normal random variable, and

$$\sigma_T^2 = \frac{1}{4}\left(2 + \frac{\kappa_4}{\sigma_0^4}\right). \tag{14}$$

Here, $\sigma_0^2 = var(\varepsilon_t)$ *as in* (A5) *and* $\kappa_4 = E[(\varepsilon_t/\sigma_0)^2] - 3$ *is the kurtosis of* ε_t.

The asymptotic behaviour of T_n under H_1 is characterized by the following Theorems.

Theorem 2 *Suppose that* H_1 *holds with* $\omega_{0,S} \neq \omega_{0,X}$. *Then, under* (A1) *to* (A8), *there is a constant* $0 < c_T < \infty$ *such that*

$$n^{-\frac{1}{2}} T_n \underset{p}{\to} c_T. \tag{15}$$

Theorem 3 *Suppose that* H_1 *holds with* $\omega_{0,S} = \omega_{0,X}$. *Also, assume that* (A1) *to* (A8) *hold and* $0 < d < \frac{1}{4}$. *Then there are constants* $0 < c_{T,1}, c_{T,2} < \infty$ *such that*

$$P\Big(c_{T,1} \leq n^{2d-\frac{1}{2}} |T_n| \leq c_{T,2}\Big) \to 1.$$

Moreover, if $d > \frac{1}{4}$, *then*

$$T_n = O_p(1).$$

Given Theorems 1, 2 and 3, critical regions at the level of significance $\alpha \in (0, 1)$ can be defined by

$$C_{\alpha;n} = P\big(T_n > \sigma_T^{-1} z_{1-\alpha}\big) \tag{16}$$

where $z_{1-\alpha}$ is the $(1-\alpha)-$ quantile of the standard normal distribution. Theorems 2 and 3 imply the following results for the power of the test.

Corollary 1 *Assume* (A1) *to* (A8), *and* H_1 *with* $\omega_{0,S} \neq \omega_{0,X}$. *Then there is a constant* $0 < q < \infty$ *such that*

$$1 - P\big(C_{\alpha,n}\big) = O\Big(n^{-\frac{1}{2}} \exp(-qn)\Big), \tag{17}$$

as $n \to \infty$.

Corollary 2 *Assume* (A1) *to* (A8), H_1 *with* $\omega_{0,S} = \omega_{0,X}$, *and* $d < 1/4$. *Then there are constants* $0 < a_1, a_2, b_1, b_2 < \infty$ *such that, as* $n \to \infty$,

$$a_1 n^{-\frac{1}{2}+2d} \exp\left(-b_1 n^{1-4d}\right) \leq 1 - P\big(C_{\alpha,n}\big) \leq a_2 n^{-\frac{1}{2}+2d} \exp\left(-b_2 n^{1-4d}\right). \tag{18}$$

Moreover, for $d > 1/4$, $1 - P(C_{\alpha,n})$ *does not converge to zero.*

Theorem 3 and Corollary 2 illustrate the difficulty of identifying a deterministic periodic component S_t when the spectral density of the noise process X_t has a pole at the same frequency. The bound for the rate at which the power converges to 1 slows down as periodic long memory, characterized by d, increases. Technically, the reason for this behaviour is that for λ_j close to $\omega_{0,X}$, the weights $1/f(\lambda_j)$ are proportional to $|\lambda_j - \omega_{0,X}|^{2d}$. The increasing value of the Fejér kernel at $\lambda_j - \omega_{0,S}$ is thus dampened by a constant time $|\lambda_j - \omega_{0,X}|^{2d}$, if $\omega_{0,S} = \omega_{0,X}$. To increase power and to obtain consistency for $d \geq \frac{1}{4}$, one may thus try to insert a weight function that compensates for the factor $1/f(\lambda_j)$, while keeping asymptotic normality of the test statistic under the null hypothesis. A natural modification of T_n is given by

$$T_{\beta;n} = T_{\beta;n}\left(\psi_X^0\right) = n^{-\frac{1}{2}} \sum_{j=1}^{m} w_\beta\left(\lambda;\omega_{0,X},\theta_0\right)\left(\frac{I\left(\lambda_j\right)}{f\left(\lambda_j;\psi_X^0\right)} - 1\right) \tag{19}$$

where

$$w_\beta\left(\lambda;\omega_{0,X},\theta_0\right) = g^\beta\left(\lambda;\omega_{0,X},\theta_0\right) 1\left\{\lambda \neq \omega_{0,X}\right\} \tag{20}$$

for some $0 \leq \beta < 1$ and $m = [n/2]$. The asymptotic distribution of $T_{\beta;n}$ under H_0 is given by

Theorem 4 *Suppose that* (A1) *to* (A8) *hold*, $0 \leq \beta < 1$ *and*

$$d < \min\left\{\frac{1}{2}, \frac{1}{4\beta}\right\}. \tag{21}$$

Then, *under* H_0,

$$T_{\beta;n} \underset{d}{\to} \sigma_T Z \tag{22}$$

where Z *is a standard normal variable and*

$$\sigma_T^2 = v_2 + v_1^2 \sigma_0^{-4} \kappa_4 \tag{23}$$

with

$$v_1 = \frac{1}{2\pi} \int_0^\pi g^\beta\left(\lambda;\omega_{0,X},\theta_0\right) d\lambda$$

and

$$v_2 = \frac{1}{2\pi} \int_0^\pi g^{2\beta}\left(\lambda;\omega_{0,X},\theta_0\right) d\lambda.$$

Under H_1, the following result can be obtained.

Theorem 5 *Assume* (A1) *to* (A8), *and* H_1 *with* $\omega_{0,S} \neq \omega_{0,X}$ *hold. Then there is a constant* $0 < c_T < \infty$ *such that*

$$n^{-\frac{1}{2}} T_{\beta;n} \underset{p}{\to} c_T. \tag{24}$$

Theorem 6 *Assume* (A1) *to* (A8), *and* H_1 *with* $\omega_{0,S} = \omega_{0,X}$. *Also, suppose that*

$$d < d_{\max} = \min\left\{\frac{1}{2}, \frac{1}{4\beta}, \frac{1}{4(1-\beta)}\right\}. \tag{25}$$

Then there are constants $0 < c_{T,1}, c_{T,2} < \infty$ *such that*

$$P\Big(c_{T,1} \leq n^{2(1-\beta)d-\frac{1}{2}} \Big| T_{\beta;n} \Big| \leq c_{T,2}\Big) \to 1. \tag{26}$$

Moreover, if $d > d_{\max}$, *then*

$$T_{\beta;n} = O_p(1).$$

Asymptotic rejection regions at the level of significance $\alpha \in (0,1)$ are defined by

$$C_{\alpha,n} = \left\{T_{\beta;n} > z_{1-\alpha}\sigma_T\right\}$$

where σ_T is given in (23). The asymptotic power of the test is characterized by the following Corollaries.

Corollary 3 *Assume* (A1) *to* (A8), *and* H_1 *with* $\omega_{0,S} \neq \omega_{0,X}$. *Then there is a constant* $0 < q < \infty$ *such that*

$$1 - P\big(C_{\alpha,n}\big) = O\Big(n^{-\frac{1}{2}} \exp\left(-qn\right)\Big), \tag{27}$$

as $n \to \infty$.

Corollary 4 *Assume* (A1) *to* (A8), (25) *and* H_1 *with* $\omega_{0,S} = \omega_{0,X}$. *Then there are constants* $0 < a_1, a_2, b_1, b_2 < \infty$ *such that, as* $n \to \infty$,

$$\begin{aligned} a_1 n^{-\frac{1}{2}+2(1-\beta)d} \exp\left(-b_1 n^{1-4(1-\beta)d}\right) \leq & 1 - P\big(C_{\alpha,n}\big) \leq a_2 n^{-\frac{1}{2}+2(1-\beta)d} \\ & \exp\left(-b_2 n^{1-4(1-\beta)d}\right). \end{aligned} \tag{28}$$

Moreover, if (25) *does not hold, then* $1 - P(C_{\alpha,n})$ *does not converge to zero.*

Remark 3 If $\kappa_4 = 0$, then the asymptotic variance of $T_{0;n}$ does not depend on unknown parameters. This is not the case for other choices of β. In this sense, $\beta = 0$ is a suitable choice in applications, provided that $d < \frac{1}{4}$. On the other hand, for $\beta \neq \frac{1}{2}$, condition (25) restricts d to the interval $0 < d < d_{\max}$ with $d_{\max} = d_{\max}(\beta)$ strictly smaller than $\frac{1}{2}$. The only value of β where $d_{\max}(\beta) = \frac{1}{2}$ is $\beta = \frac{1}{2}$. In view of

the fact that d is unknown in applications, and at the same time the rate improves monotonically in β, one may prefer to use $\beta = \frac{1}{2}$. Note also that, if $\kappa_4 = 0$, then the asymptotic variance of $T_{\frac{1}{2};n}$ simplifies to

$$\sigma_T^2 = \frac{\sigma_X^2 \sigma_\varepsilon^{-2}}{4\pi}.$$

Remark 4 The results can be generalized to the situation where the spectral density of f_X has several poles at frequencies $\omega \in \Omega_X = \{\omega_{1,X}, ..., \omega_{p_X,X}\}$, and $dF_S(\omega) > 0$ for $\omega \in \Omega_S = \{\omega_{1,S}, ..., \omega_{p_S,S}\}$.

Remark 5 For numerical stability, one may avoid using frequencies that are very close to the pole of f_X, without changing the asymptotic distribution of $T_{\beta;n}$. Given a sequence M_n such that $M_n \to \infty$ and $M_n/n \to 0$, this can be achieved by omitting Fourier frequencies with $|\lambda_j - \omega_{0,X}| \leq 2\pi M_n/n$ from the sum in (19).

4 Testing with unknown parameters

For the case where ψ and $\omega_{0,S}$ are unknown, the following algorithm can be used:

- Step 1: Let $1 \leq j_{0,n} \leq m = [n/2]$ be the smallest integer such that

$$I_{Y,n}\left(\lambda_{j_{0,n}}\right) = \max_{j=1,...,m} I_{Y,n}\left(\lambda_j\right),$$

and set

$$\hat{\omega}_{0,S} = \lambda_{j_{0,n}}. \tag{29}$$

- Step 2: Let $M_n \in \mathbb{N}$ such that $M_n \to \infty$, $M_n/n \to 0$,

$$\begin{aligned} J_n =& J_n\left(\hat{\omega}_{0,S}\right) = \left\{j_{0,n} - M_n, j_{0,n} - M_n + 1, ..., j_{0,n} + M_n\right\}, \\ \Lambda_n\left(\hat{\omega}_{0,S}\right) =& \left\{ \lambda_j = \frac{2\pi j}{n}, j \in J_n\left(\hat{\omega}_{0,S}\right) \right\}, \\ Q_{n,Y}^*(\omega, \theta) =& \frac{1}{n} \sum_{\substack{j=1 \\ j \notin J_n}}^{m} \frac{I_{Y,n}\left(\lambda_j\right)}{g\left(\lambda_j; \omega, \theta\right)} \end{aligned}$$

and

$$\left(\hat{\omega}_{0,X}, \hat{\theta}\right) = \arg\min_{(\omega,\theta)} Q_{n,Y}^*(\omega, \theta). \tag{30}$$

Consistency of $\hat{\omega}_{0,S}$ under H_1 follows from the properties of the Féjer kernel. More specifically, $\hat{\omega}_{0,S} - \omega_{0,S} = O_p(n^{-1})$. With respect to $\hat{\omega}_{0,X}$ and $\hat{\theta}$, the following holds:

Theorem 7 *Suppose that* (A1) *to* (A8) *hold. Let* $\hat{\omega}_{0,X}$ *be defined by* (30). *Then, under* H_0 *and under* H_1,

$$\hat{\omega}_{0,X} = \omega_{0,X} + O_p\big(n^{-1}\big), \tag{31}$$

and

$$\sqrt{n}\big(\hat{\theta} - \theta^0\big) \underset{d}{\to} \zeta \tag{32}$$

where ζ *is a normal random variable with expected value zero and covariance matrix*

$$\Sigma_\zeta = V^{-1}$$

with

$$V_{ij} = \frac{1}{4\pi}\int_{-\pi}^{\pi} \frac{\partial}{\partial\theta}\log g\big(\lambda;\omega_{0,X},\theta\big)\Big[\frac{\partial}{\partial\theta}\log g\big(\lambda;\omega_{0,X},\theta\big)\Big]^T d\lambda \mid_{\theta=\theta^0}.$$

Theorem 7 implies that the unknown parameters in $T_{\beta;n}$ and σ_T^2 can be replaced by their estimates without changing the asymptotic distribution of $T_{\beta;n}$.

Remark 6 In the definition of $(\hat{\omega}_{0,X}, \hat{\theta})$, the set of frequencies $\Lambda_n(\hat{\omega}_{0,S})$ is omitted. Here, the essential condition is $M_n/n \to 0$. Applying Theorem 4.2 in Giraitis et al. (2001) then leads to the result that $Q^*_{n,Y}(\omega,\theta)$ and $Q_{n,Y} = \sum_{j=1}^m I_{Y,n}(\lambda_j)/g(\lambda_j;\omega,\theta)$ are asymptotically equivalent in the sense that $\sqrt{n}(Q^*_{n,Y} - Q_{n,Y}) \to_p 0$. Therefore, the asymptotic results in Theorem 7 are not affected.

5 Simulations and data examples

5.1 Simulations

We consider simulations of model (3) with $S_t = b\sin\omega_{0,S}t$. The stationary process X_t is generated by a Gegenbauer process process with a pole at $\omega_{0,X} = 1$. Two alternatives are considered: a) $H_{1,1}$: $b = 4$ with $\omega_{0,S} = 1$, b) $H_{1,2}$: $b = 4$ with $\omega_{0,S} = 3$. The long-memory parameter d and the sample sizes are set to d =0.1, 0.2, 0.3, 0.4, and n =200, 400 and 800 respectively. For each combination of parameters and series length, $N = 1000$ simulated series were generated. For each series, $T_{0;n}$ and $T_{\frac{1}{2};n}$ were computed and compared to the 95%− quantiles of the corresponding $N(0,\sigma_T^2)$ distribution. For the case with unknown parameters, the method defined in the

Table 1 Simulated rejection probabilities based on T_0 and $T_{1/2}$ respectively, when parameters are known

H_0						
	T_0			$T_{1/2}$		
d	n =200	400	800	200	400	800
0.1	0.05	0.04	0.04	0.05	0.05	0.04
0.2	0.07	0.07	0.07	0.03	0.04	0.03
0.3	0.07	0.07	0.07	0.09	0.10	0.05
0.4	0.15	0.14	0.08	0.13	0.11	0.09
H_1 with $\omega_X = 1, \omega_S = 1$						
0.1	1	1	1	1	1	1
0.2	1	1	1	1	1	1
0.3	1	1	1	1	1	1
0.4	0.91	0.94	0.85	0.99	0.97	0.99
H_1 with $\omega_X = 1, \omega_S = 3$						
0.1	1	1	1	1	1	1
0.2	1	1	1	1	1	1
0.3	1	1	1	1	1	1
0.4	1	1	1	1	1	1

Table 2 Simulated rejection probabilities based on T_0 and $T_{1/2}$ respectively, when parameters are estimated. Also given are the simulated means of $\hat{d}$, $\hat{\omega}_X$ and $\hat{\omega}_S$

H_0									
	T_0			$T_{1/2}$			$\hat{d}, \hat{\omega}_X, \hat{\omega}_S$		
0.1	0.01	0	0	0	0	0	0.09, 1.07, 1.20	0.07, 1.02, 1.02	0.08, 0.99, 1.11
0.2	0.03	0	0.02	0	0	0	0.18, 1.01, 0.99	0.17, 0.99, 1.00	0.18, 1.01, 0.99
0.3	0.07	0.07	0	0	0	0	0.25, 0.99, 1.00	0.26, 1.00, 1.00	0.28, 1.00, 1.00
0.4	0.19	0.12	0.03	0	0.01	0.01	0.35, 0.99, 1.00	0.37, 0.99, 1.00	0.39, 1.00, 1.00
H_1 with $\omega_X = 1, \omega_S = 1$									
0.1	1	0.94	0.99	0.86	0.84	0.99	0.26, 0.99, 1.01	0.30, 0.99, 1.01	0.21, 1.01, 1.00
0.2	0.97	0.77	0.82	0.72	0.79	0.93	0.30, 0.99, 1.01	0.35, 0.99, 1.01	0.31, 1.01, 1.00
0.3	0.95	0.69	0.59	0.53	0.76	0.85	0.35, 0.99, 1.01	0.39, 0.99, 1.01	0.37, 1.01, 1.00
0.4	0.72	0.48	0.54	0.15	0.46	0.46	0.42, 0.99, 1.01	0.45, 0.99, 1.01	0.44, 1.01, 1.00
H_1 with $\omega_X = 1, \omega_S = 3$									
0.1	1	1	1	1	1	1	0.23, 2.83, 3.02	0.01, 2.67, 3.00	0, 2.84, 3.00
0.2	1	1	1	1	1	1	0.20, 2.83, 3.01	0.02, 2.43, 3.00	0.01, 2.74, 3.00
0.3	1	1	1	1	1	1	0.15, 2.83, 3.02	0.03, 2.17, 3.00	0.02, 2.40, 3.00
0.4	1	1	1	1	1	1	0.09, 2.80, 3.00	0.15, 1.25, 3.00	0.12, 1.59, 3.00

previous section was applied with $M_n = [\frac{1}{2} \log \log n]$. The results are summarized in Tables 1 and 2. For the case where parameters are estimated, the simulated sampe means of $\hat{d}$, $\hat{\omega}_{0,X}$ and $\hat{\omega}_{0,S}$ are also given (Table 2).

In the case where parameters are known (Table 1), the rejection probabilities under H_0 converge reasonably fast to the nominal level of significance. For very strong long memory ($d = 0.4$) convergence to the nominal level is somewhat slower. With respect to power, one obtains almost a perfect rejection rate in the case of known parameters, even for $d = 0.4$. Also, as expected, generally $T_{1/2}$ appears to have higher power against H_1, as specified here. In the situation where parameters are estimated (Table 2), the test appears to be on the conservative side for small sample sizes, i.e. the level of the test is generally lower than the nominal one. With respect to power, the situation is more complicated. For very weak long memory, with $d = 0.1$, the rejection rate is again almost perfect. For $d \geq 0.2$, this remains to be true for the second alternative $H_{1,2}$ where $\omega_{0,S} \neq \omega_{0,X}$. In comparison, simulated rejection frequencies tend to be lower for the first alternative $H_{1,1}$. This illustrates that distinguishing stochastic from deterministic periodicity is more difficult when $\omega_{0,S} = \omega_{0,X}$. Finally note that in the case with $\omega_{0,S} \neq \omega_{0,X}$, there is a relatively large bias in the estimates of $\omega_{0,X}$ and d. For a small minority of the simulated sample paths, the estimated values $\hat{\omega}_{0,X}$ indeed turned out to be closer to $\omega_{0,S} = 3$ rather than $\omega_{0,X} = 1$. This is in particular the case, when d is small. This also illustrates the difficulty of distinguishing deterministic from stochastic periodicity.

5.2 Data example

Weakness of respiratory muscles is common in various acute and chronic diseases like chronic obstructive pulmonary disease, SarsCoV2 or during and following intensive care medicine (Kabitz et al. 2007 and Regmi et al. 2023). Respiratory muscle training aims at improving respiratory muscle strength and endurance through three distinct training methods: inspiratory pressure threshold loading, flow resistive loading and voluntary isocapnic hyperpnea (Walterspacher et al. 2018). In the study by Walterspacher et al. (2018) those three distinct ways of respiratory muscle training were studied in order to understand the different modes of activation of the three major inspiratory muscle groups: diaphragm, intercostal muscles and cervical muscles. This data set was used for the current statistical analysis. To make time series analysis feasible, only subjects were considered where the observed series were long enough. Compared to the original study by Walterspacher et al. (2018), the number of subjects therefore reduced from 41 to 28.

Previous analysis of the data has shown that inspiratory pressure threshold loading lead to predominant activation of the major respiratory muscle, the diaphragm (Walterspacher et al. 2018). Healthy subjects were asked to perform various respiratory exercises. The activity of respiratory muscles was measured by surface electromyography (sEMG). For illustrative purposes, we focus on measurements of the diaphragm obtained from the right electrode. Denote by $z(s_j)$ the sEMG measurement at time s_j. The original measurements were recorded at a time resolution of 0.01 seconds, i.e. $s_j = j \cdot 0.01$ seconds. The quantity of interest is "respiratory effort" of the

specific muscle group, which may be approximated by the square of the sEMG-signal. To exclude very high frequencies, in particular effects of the heart beat, $z^2_{Dia}(s_j)$ is first aggregated to a time resolution of 1 second. Moreover, to symmetrize the series, a logarithmic transformation is applied. Thus, we consider

$$y_t = \log\left(\sum_{j\in I(t)} z^2_{Dia}(s_j)\right)(t = 1, 2, ...)$$

where $I(t) = \{100(t-1)+1 \le j \le 100t\}$. Walterspacher et al. (2018) considered seven basic types of respiratory exercises for respiratory muscle EMG assessment (denoted according to the devices used): *MVV , TLC, Sniff , PImax,* as measures of maximal muscle innervation tests, and *SpiroTiger , RespiFit, POWERbreathe*, as respiratory muscle training tests.

To simplify the presentation, we compare two trainings that were carried out in a similar fashion, namely *SpiroTiger* and *POWERbreathe (PB)*. A brief description of the exercises can be given as follows: 1) *SpiroTiger*: isocapnic voluntary hyperventilation is a type of respiratory muscle training that requires the subjects to ventilate at a high proportion of their maximum voluntary ventilation for a fixed period. In this set-up subjects were asked to breathe for 1min with 30 sec break; 2) *POWERbreathe*: subjects are asked to inspire against an occluded airway that opened at 80% of the individual maximal inspiratory muscle strength. Two bouts of each 5 inspiratory efforts with a 30 sec break were used in this training session.

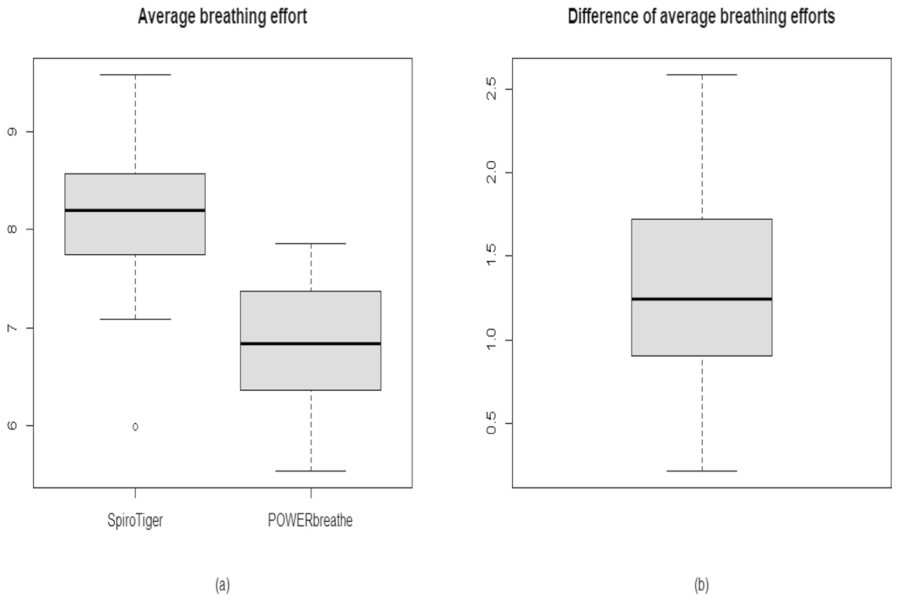

Fig. 3 Average breathing effort during a *SpiroTiger* and a *POWERbreathe* exercise respectively (**a**), for 28 subjects. **b** Shows a boxplot of the (paired) differences $\Delta\bar{y}(j) = \bar{y}_{SpiroTiger}(j) - \bar{y}_{POWERbreathe}(j)$

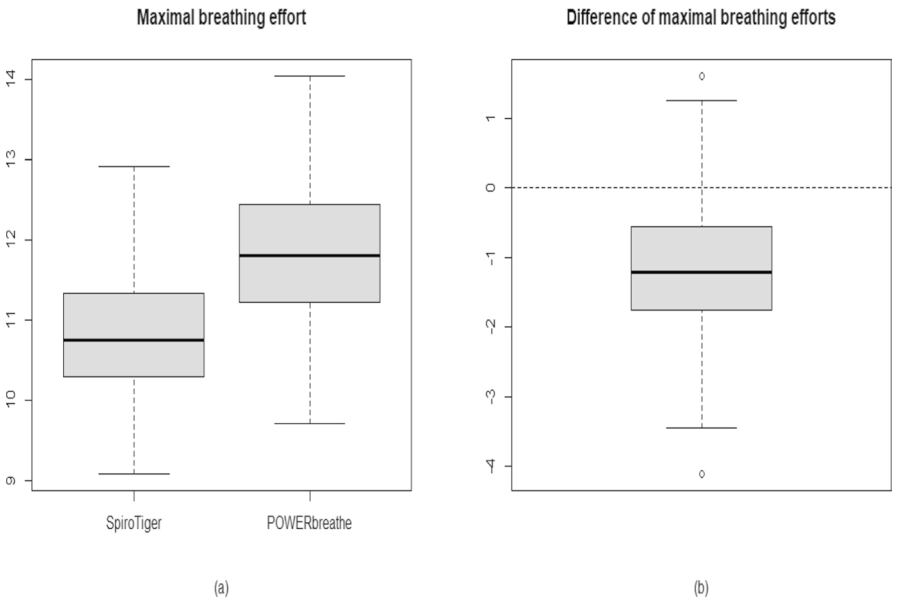

Fig. 4 Maximal breathing effort during a *SpiroTiger* and a *POWERbreathe* exercise respectively (**a**), for 28 subjects. **b** Shows a boxplot of the (paired) differences $\Delta\bar{y}(j) = \bar{y}_{SpiroTiger}(j) - \bar{y}_{POWERbreathe}(j)$

Figure 3a shows boxplots of sample means $\bar{y}_{SpiroTiger}(j)$ and $\bar{y}_{PB}(j)$ for 28 subjects ($j = 1, ..., 28$). The differences $\Delta\bar{y}(j) = \bar{y}_{SpiroTiger}(j) - \bar{y}_{PB}(j)$ are displayed in Fig. 3b. Denoting by $\mu_{SpiroTiger}$ and μ_{PB} the corresponding expected values, a Wilcoxon signed-rank test of $H_0 : \mu_{SpiroTiger} \leq \mu_{PB}$ against $H_1 : \mu_{SpiroTiger} > \mu_{PB}$ yields a p-value smaller than 10^{-8}. Thus, there is strong evidence for *SpiroTiger* generally leading to a higher average breathing effort of the diaphragm. On the other hand, it should be noted that different results are obtained when high quantiles of the effort distributions are compared. For instance, Fig. 4a shows boxplots of the maximal effort. The within subject differences of the maxima are shown in Fig. 4b. In this comparison, *POWERbreathe* turns out to be clearly more effective than *SpiroTiger*, with a p-value of the paired Wilcoxon signed-rank test below 0.0002. This confirms the findings of Walterspacher et al. (2018). The difference between the results for the average and the maximal breathing effort can be explained by the design of the exercises: *SpiroTiger* aims at improving endurance, whereas *POWERbreathe* is designed as a strength training.

In a next step, we take a closer look at the individual time series. Breathing exercises intrinsically contain strong periodic features that are however not necessarily exactly periodic. We are therefore interested in testing whether the observed time series y_t ($t = 1, 2, ...$) contain a deterministic periodic component or whether stochastic periodicity is prevalent. For each subject, the algorithm in Sect. 4 was applied to each series $y_t(j)$ ($t = 1, 2, ...$), with $M_n = [\frac{1}{2} \log \log n]$. A typical pair of series is shown in Figs. 1a, (*SpiroTiger)* and 2a (*POWERbreathe)*.

The measurements in Fig. 1a were taken during the first 136 s (i.e. $n = 136$) of a *SpiroTiger*-exercise. Figure 2a shows, for the same subject, measurements during the first 112 s (i.e. $n = 112$) of a *POWERbreathe*-exercise. The different sample sizes are due to the different duration of the exercises. The corresponding periodograms are displayed in Figs. 1c and 2c. The solid and the dotted vertical lines mark the location of $\hat{\omega}_S$ and $\hat{\omega}_X$ respectively. Figure 1c (*SpiroTiger*) shows a distinct maximum, indicating a strong periodic component. However, $\hat{\omega}_S = 0.65$ and $\hat{\omega}_X = 0.79$ are very close together. This makes it difficult to tell whether a deterministic periodic component is present. The parameter estimates and the test statistics are: $\hat{d} = 0.11$ with a 95%−confidence interval of [0.04, 0.18], $T_0 = 0.92$ and $T_{1/2} = 1.20$. The corresponding p-values are 0.18 for T_0 and 0.12 for $T_{1/2}$ respectively. For *POWERbreathe*, Fig. 2c shows two very distinct peaks around $\hat{\omega}_X = 0.56$ and $\hat{\omega}_S = 1.01$ respectively. Here, $\hat{d} = 0.30$ with a 95%−confidence interval of [0.20, 0.40], $T_0 = 2.23$ and $T_{1/2} = 2.25$. The p-values for T_0 and $T_{1/2}$, are 0.01. Thus, in spite of stronger periodic long memory and a smaller sample size, there is much stronger evidence for a deterministic periodic component. This confirms the visual impression that the maximum around $\hat{\omega}_S$ in Fig. 2c is quite isolated, thus indicating a deterministic component, whereas the peak around $\hat{\omega}_X$ is more dispersed.

The test statistics T_0 and $T_{1/2}$ may be interpreted as descriptive measures of the relative strength of potential deterministic periodic components. The same analysis was carried out for all 28 subjects. Boxplots of p-values based on T_0 and $T_{1/2}$ are shown in Fig. 5a and b respectively. The comparison indicates that, in general, for the *POWERbreathe* training, breathing effort tends to be more regular. A corresponding one-sided paired Wilcoxon signed-rank test yields a p-value of 0.04

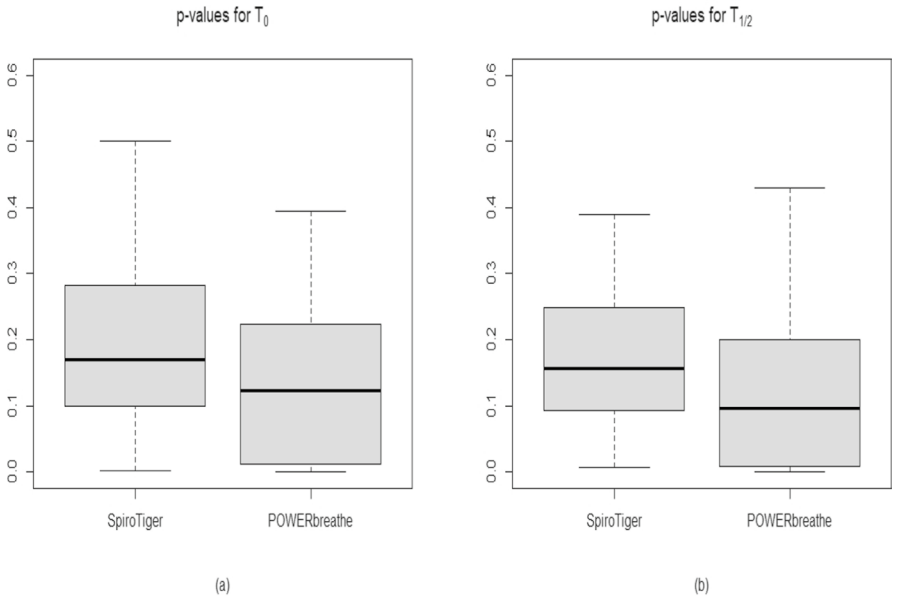

Fig. 5 *P* values for T_0 (**a**) and $T_{1/2}$ (**b**) for the *SpiroTiger*- and *POWERbreathe*-exercises

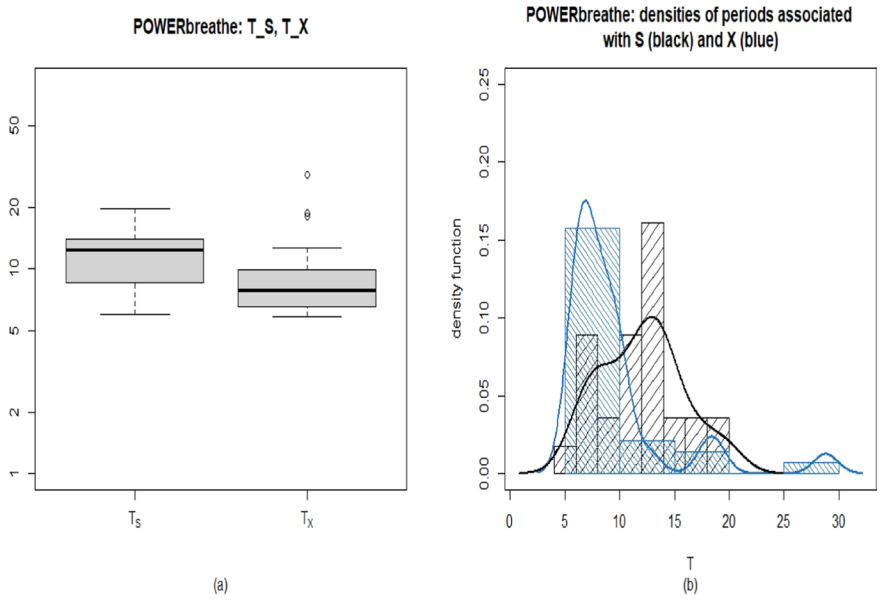

Fig. 6 Boxplots of $T_S = 2\pi/\hat{\omega}_S$ and $T_X = 2\pi/\hat{\omega}_X$ (**a**) for *POWERbreathe*. **b** Shows kernel density estimates of the distributions of T_S (black) and T_X (blue) respectively (colour figure online)

for T_0- and 0.02 for $T_{1/2}-$p-values. It is also interesting to compare the periods $\hat{T}_S = 2\pi/\hat{\omega}_{0,S}$ and $\hat{T}_X = 2\pi/\hat{\omega}_{0,X}$ associated with the estimated frequencies $\hat{\omega}_{0,S}$ and $\hat{\omega}_{0,X}$. For *POWERbreathe*, the expected value of $\hat{T}_S$ is significantly higher than the expected value of $\hat{T}_X$ (Fig. 6a). The p-value of the corresponding one-sided Wilcoxon signed-rank test turns out to be 0.001. In contrast, for *SpiroTiger*, this is not the case. Figure 6b also shows estimated density functions of $\hat{T}_S$ and $\hat{T}_X$ for *POWERbreathe* .

In summary one may conclude that, in comparison with *POWERbreathe*, the *SpiroTiger*-exercise generally leads 1) to a higher average breathing effort of the diaphragm, and 2) to less regular fluctuations in breathing effort. Moreover, for *POWERbreathe*, the potentially deterministic periodic component tends to oscillate at a lower frequency than stochastic periodic long memory.

6 Final remarks

In this paper we considered simple tests for a jump in the spectral distribution function, under the assumption of periodic long memory. As expected, this task is more difficult when the location of the jump coincides with the location of the pole of the spectral density. The proposed method can be generalized to situations with more than one jump of the spectral distribution function and/or several poles of the spectral density. Though a generalization is straightforward in principle, a detailed development of such methods needs some care in order to obtain feasible solutions that perform well for finite samples. Note in particular

that, in general, a periodic function S_t has an infinite Fourier series representation. Combined with the effect of aliasing, the detection of peaks in the spectrum that are caused by S_t is a difficult task in general. These and related questions in the context of noise processes that exhibit periodic long memory with multiple peaks are formidable tasks to be addressed in future research.

Appendix

Proofs

Proof of Theorem 1 We use the notation $m_n = [n/2]$ for the integer part of $n/2$. Let $j_{0,n}$ be such that

$$\left|\lambda_{j_{0,n}} - \omega_{0,X}\right| = \min\left\{\left|\lambda_j - \omega_{0,X}\right|, 1 \le j \le m_n\right\}.$$

Also, define a triangular array of coefficients

$$b_{j,n} = n^{-\frac{1}{2}} \ (1 \le j \le m_n, n = 1, 2, ...).$$

Then T_n can be written as

$$T_n(\omega, \theta) = \sum_{\substack{j=1 \\ j \ne j_{0,n}}}^{[n/2]} b_{j,n}\left(\frac{I(\lambda_j)}{f(\lambda_j;\psi)} - 1\right) + b_{j_{0,n}}\left(\frac{I\left(\lambda_{j_{0,n}}\right)}{f\left(\lambda_{j_{0,n}};\psi\right)} - 1\right).$$

Lemma 4.1 in Giraitis et al. (2001) implies $T_n \to_d \sigma_T Z$ with

$$\sigma_T^2 = v_2 + v_1^2 \sigma_0^{-4} \kappa_4$$

where

$$v_1 = \lim_{n\to\infty} n^{-\frac{1}{2}} \sum_{j=1}^{m_n} b_{j,n} = \lim_{n\to\infty} \frac{m_n}{n} = \frac{1}{2}$$

and

$$v_2 = \lim_{n\to\infty} \sum_{j=1}^{m_n} b_{j,n}^2 = \lim_{n\to\infty} \frac{m_n}{n} = \frac{1}{2}.$$

□

Proof of Theorem 2 Under H_1, $Y_t = S_t + X_t = \alpha_1 \cos\omega_{0,S}t + \alpha_2 \sin\omega_{0,S}t + X_t$ where $\max\{|\alpha_1|, |\alpha_2|\} > 0$. Since we are only interested in the order of magnitude of T_n, we may consider without loss of generality $S_t = \exp(-it\omega_{0,S})$ instead. Then

$$I(\lambda) = \frac{1}{2\pi n}\left|\sum_{t=1}^{n}\left(S_t + X_t\right)e^{it\lambda}\right|^2 = I_S(\lambda) + I_{SX}(\lambda) + \bar{I}_{SX}(\lambda) + I_X(\lambda)$$

where

$$I_S(\lambda) = \frac{1}{2\pi n}\left|\sum_{t=1}^{n} e^{it(\lambda-\omega_{0,S})}\right|^2, I_X(\lambda) = \frac{1}{2\pi n}\left|\sum_{t=1}^{n} X_t e^{it\lambda}\right|^2,$$
$$I_{SX}(\lambda) = \frac{1}{2\pi n}\sum_{t_1,t_2=1}^{n} X_{t_2} e^{i\lambda(t_1-t_2)}e^{-it_1\omega_{0,S}}.$$

It is straightforward to see that $I_X = o_p(I_S)$ and $|I_{SX}| = o_p(I_S)$. For I_S, we have

$$I_S(\lambda) = \frac{1}{2\pi n}\left|\sum_{t=1}^{n}\exp(i\left(\lambda-\omega_{0,S}\right)t)\right|^2 = \frac{1}{2\pi n}\left|\frac{\sin\left(\frac{n}{2}\left(\lambda-\omega_{0,S}\right)\right)}{\sin\left(\frac{1}{2}\left(\lambda-\omega_{0,S}\right)\right)}\right|^2$$
$$= \frac{1}{2\pi}F_n\left(\lambda-\omega_{0,S}\right)$$

where F_n denotes the Fejér kernel. As a result,

$$T_n = A_n \cdot \left(1 + o_p(1)\right)$$

where

$$A_n = n^{\frac{1}{2}}\frac{1}{(2\pi)^2}\sum_{j=1}^{m_n}\frac{F_n\left(\lambda_j-\omega_{0,S}\right)}{f\left(\lambda_j;\psi\right)}\frac{2\pi}{n}$$
$$\sim n^{\frac{1}{2}}\frac{1}{(2\pi)^2}\int_0^{\pi} f^{-1}(\lambda)F_n\left(\lambda-\omega_{0,S}\right)d\lambda$$
$$\sim n^{\frac{1}{2}}\frac{1}{(2\pi)^2}f^{-1}\left(\omega_{0,S}\right) = n^{\frac{1}{2}}c_T.$$

□

Proof of Theorem 3 We use the same notation

$$I(\lambda) = \frac{1}{2\pi n}\left|\sum_{t=1}^{n}\left(S_t + X_t\right)e^{it\lambda}\right|^2 = I_S(\lambda) + I_{SX}(\lambda) + \bar{I}_{SX}(\lambda) + I_X(\lambda)$$

as in the proof of Theorem 2. Let $j_{0,n}$ be such that

$$\left|\lambda_{j_{0,n}} - \omega_{0,X}\right| = \min\left\{\left|\lambda_j - \omega_{0,X}\right|, 1 \le j \le m_n\right\}.$$

As in Theorem 2, it is sufficient to consider $S_t = \exp(-it\omega_{0,S})$ and

$$I_S(\lambda) = \frac{1}{2\pi n}\left|\sum_{t=1}^{n} e^{it(\lambda-\omega_{0,S})}\right|^2 = \frac{1}{2\pi}F_n\left(\lambda - \omega_{0,S}\right).$$

Due to the properties of the Fejér kernel and $\omega_{0,S} = \omega_{0,X}$, we have

$$\begin{aligned} A_n &= n^{\frac{1}{2}}\frac{1}{(2\pi)^2}\sum_{j=1}^{m_n}\frac{F_n\left(\lambda_j - \omega_{0,S}\right)}{f\left(\lambda_j;\psi\right)}\frac{2\pi}{n} \\ &= n^{\frac{1}{2}}\left(\int\frac{F_n(\lambda)}{f(\lambda;\psi)}d\lambda + r_n\right) \end{aligned}$$

where

$$\int F_n(\lambda)f(\lambda;\psi)d\lambda = \lim_{\lambda\to\omega_{0,X}}\frac{1}{f(\lambda;\psi)} = 0$$

and

$$\begin{aligned} r_n = &\sum_{j=1}^{m_n}\frac{F_n\left(\lambda_j^* - \omega_{0,X}\right)f'\left(\lambda_j^*;\psi\right)}{f^2\left(\lambda_j^*;\psi\right)}\frac{2\pi}{n} \\ &+ \sum_{j=1}^{m_n}\frac{F_n'\left(\lambda_j^* - \omega_{0,X}\right)}{f\left(\lambda_j^*;\psi\right)}\frac{2\pi}{n} \end{aligned}$$

with $|\lambda_j^* - \lambda_j| \le 2\pi/n$. The upper and lower bound for $\sqrt{n}r_n$ then follows from

$$n^{-1}\left|\frac{F_n'\left(2\pi cn^{-1}\right)}{f\left(\omega_{0,X} + 2\pi cn^{-1};\psi\right)}\right| \sim c_1 \cdot n^{-2d}$$

and

$$n^{-1}\left|\frac{F_n\left(2\pi cn^{-1}\right)f'\left(\omega_{0,X} + 2\pi cn^{-1};\psi\right)}{f^2\left(\omega_{0,X} + 2\pi cn^{-1};\psi\right)}\right| \sim c_2 n^{-2d},$$

where $0 < c, c_1, c_2 < \infty$. □

Proof of Corollary 1 The result follows from

$$\frac{z}{z^2+1}\varphi(z) \le 1-\Phi(z) \le \frac{1}{z}\varphi(z)$$

(see e.g. Grimmett and Stirzaker 2020), and Theorem 3. □

Proof of Corollary 2 The result follows from Theorem 3, and

$$\frac{z}{z^2+1}\varphi(z) \le 1-\Phi(z) \le \frac{1}{z}\varphi(z).$$

□

Proof of Theorem 4 Let $j_{0,n}$ be such that

$$\left|\lambda_{j_{0,n}} - \omega_{0,X}\right| = \min\left\{\left|\lambda_j - \omega_{0,X}\right|, 1 \le j \le m_n\right\}.$$

Also, define a triangular array of coefficients

$$b_{j,n} = n^{-\frac{1}{2}} h\left(\lambda_j\right) \ (1 \le j \le m_n, n = 1, 2, ...)$$

where $h(\lambda) = f^{\beta}(\lambda;\psi)$. Then

$$T_{\beta;n}(\omega,\theta) = \sum_{j=1}^{[n/2]} b_{j,n}\left(\frac{I\left(\lambda_j\right)}{f\left(\lambda_j;\psi\right)} - 1\right).$$

Under the given assumptions, there exists a suitable constant $0 < C < \infty$ such that

$$\sup_{\lambda:|\lambda-\omega_{0,X}|\ge\pi/n} |h(\lambda)| = \sup_{\lambda:|\lambda-\omega_{0,X}|\ge\pi/n} \left|f^{\beta}(\lambda)\right| \le C\left|\lambda-\omega_{0,X}\right|^{-2\beta d}$$

and

$$\sup_{\lambda:|\lambda-\omega_{0,X}|\ge\pi/n} \left|\frac{d}{d\lambda}h(\lambda)\right| = \sup_{\lambda:|\lambda-\omega_{0,X}|\ge\pi/n} \left|f^{\beta-1}(\lambda;\psi)\frac{d}{d\lambda}f(\lambda;\psi)\right|$$
$$\le C\left|\lambda-\omega_{0,X}\right|^{-(2d\beta+1)}$$

uniformly in $|\lambda - \omega_{0,X}| \ge \pi/n$. Note that $0 < d < \min\{\frac{1}{2}, \frac{1}{4\beta}\}$ imply

$$2\beta d < \frac{1}{2}, 2\beta d + 1 < \frac{3}{2},$$

and

$$v_1 = \lim_{n\to\infty} n^{-\frac{1}{2}} \sum_{\substack{j=1 \\ j\neq j_{0,n}}} b_{j,n} = \frac{1}{2\pi}\int_0^\pi f^{\beta}(\lambda;\psi)d\lambda < \infty,$$

$$v_2 = \lim_{n\to\infty} \sum_{\substack{j=1 \\ j\neq j_{0,n}}} b_{j,n}^2 = \frac{1}{2\pi}\int_0^\pi f^{2\beta}(\lambda;\psi)d\lambda < \infty.$$

Theorem 4.2 in Giraitis et al. (2001) then implies

$$T_n \underset{d}{\to} N\left(0, \sigma_T^2\right)$$

with

$$\sigma_T^2 = v_2 + v_1^2\sigma_0^{-4}\kappa_4.$$

□

Proof of Theorem 5 The proof is analogous to Theorem 2. □

Proof of Theorem 6 The proof is analogous to Theorem 3. □

Proof of Corollary 3 The result follows from Theorem 5, and

$$\frac{z}{z^2+1}\varphi(z) \leq 1 - \Phi(z) \leq \frac{1}{z}\varphi(z).$$

□

Proof of Corollary 4 The result follows from Theorem 6, and

$$\frac{z}{z^2+1}\varphi(z) \leq 1 - \Phi(z) \leq \frac{1}{z}\varphi(z).$$

□

Proof of Theorem 7 First assume that H_0 holds. Since $\hat{\omega}_{0,S} = \omega_{0,X} + O_p(n^{-1})$ and $M_n \to \infty$, we obtain

$$P\left(\omega_{0,X} \in \Lambda_n\left(\hat{\omega}_{0,S}\right)\right) \to 1.$$

Let $j_{0,n}(\omega_{0,X}) = \arg\min_{j=1,\ldots,m} |\lambda_j - \omega_{0,X}|$,

$$J_{n,K}\left(\omega_{0,X}\right) = \left\{j_{0,n}\left(\omega_{0,X}\right) - KM_n, j_{0,n} - KM_n + 1, \ldots, j_{0,n}\left(\omega_{0,X}\right) + KM_n\right\},$$

and

$$\Lambda_{n,K}(\omega_{0,X}) = \left\{ \lambda_j = \frac{2\pi j}{n}, j \in J_{n,K}(\omega_{0,X}) \right\}.$$

Then, for any $K > 0$ there is a $\tilde{K}$ large enough such that

$$P\left(\Lambda_{n,K}(\hat{\omega}_{0,S}) \subseteq \Lambda_{n,\tilde{K}}(\omega_{0,X})\right) \to 1. \tag{33}$$

Now, define

$$S_n = n^{-\frac{1}{2}} \sum_{j=1}^{m} \left(\frac{I(\lambda_j)}{f(\lambda;\sigma^2,\psi)} - 1 \right), S_n^* = n^{-\frac{1}{2}} \sum_{\substack{j=1 \\ j \notin J_{n,\tilde{K}}(\omega_{0,X})}}^{m} \left(\frac{I(\lambda_j)}{f(\lambda;\psi)} - 1 \right)$$

and

$$R_n(\omega_{0,S}) = S_n - S_n^* = n^{-\frac{1}{2}} \sum_{j \in J_{n,\tilde{K}}(\omega_{0,X})} \left(\frac{I(\lambda_j)}{f(\lambda;\psi)} - 1 \right)$$

Then,

$$R_n(\omega_{0,S}) = \sum_{j=1}^{m} b_{j,n} \left(\frac{I(\lambda_j)}{f(\lambda;\psi)} - 1 \right)$$

where the coefficients

$$b_{j,n} = n^{-\frac{1}{2}} 1\left\{ \left| \lambda_j - \omega_{0,S} \right| \le \frac{2\pi \tilde{K} M_n}{n} \right\}$$

can be written as

$$b_{j,n}(\omega_{0,X}) = n^{-\frac{1}{2}} h_n(\lambda_j)$$

with

$$h_n(\lambda_j) = 1\left\{ \left| \lambda_j - \omega_{0,X} \right| \le \frac{2\pi \tilde{K} M_n}{n} \right\}.$$

Since $M_n/n \to 0$, h_n converges to the zero function. Theorem 4.2 in Giraitis et al. (2001) then implies $R_n(\omega_{0,X}) \to_p 0$. This implies $R_n(\hat{\omega}_{0,S}) \to_p 0$ (due to (33), and (32). Analogous arguments lead to $\hat{\omega}_{0,X} - \omega_{0,X} = O_p(n^{-1})$ where $\hat{\omega}_{0,X}$ is defined by (30). Finally, the consistency result under H_1 follows from the properties of the Fejér kernel. □

Acknowledgements We would like to thank the associate editor and the referees for their constructive comments that helped to improve the presentation of the results.

Funding Open Access funding enabled and organized by Projekt DEAL.

References

Alomari, H.M., Ayache, A., Fradon, M., Olenko, A.: Estimation of cyclic long-memory parameters. Scand. J. Stat. **47**(1), 104–33 (2020)

Anděl, J.: Long memory time series models. Kybernetika **22**(2), 105–123 (1986)

Arteche, J.: Exact local Whittle estimation in long memory time series with multiple poles. Econom. Theory **36**(6), 1064–1098 (2020)

Arteche, J., Robinson, P.M.: Semiparametric inferene in seasonal and cyclical long memory processes. J. Time Ser. Anal. **21**, 1–25 (2000)

Ayache, A., Fradon, M., Nanayakkara, R., Olenko, A.: Asymptotic normality of simultaneous estimators of cyclic long-memory processes. Electron. J. Stat. **16**(1), 84–115 (2022)

Beaumont, P.M., Smallwood, A.D.: Inference for estimators of generalized long memory processes. Commun. Stat. Simul. Comput. (2022). https://doi.org/10.1080/03610918.2021.2007399

Becker, A., Finger, P., Meyer-Christoffer, A., Rudolf, B., Schamm, K., Schneider, U., Ziese, M.: A description of the global land-surface precipitation data products of the global precipitation climatology centre with sample applications including centennial (trend) analysis from 1901-present. Earth Syst. Sci. Data **5**, 71–99 (2013). https://doi.org/10.5194/essd-5-71-2013

Beran, J., Feng, Y., Ghosh, S., Kulik, R.: Long-Memory Processes—Probabilistic Properties and Statistical Methods. Springer, New York/Heidelberg (2013)

Beran, J., Steffens, B., Ghosh, S.: On local trigonometric regression under dependence. J. Time Ser. Anal. **39**(4), 592–617 (2018)

Box, G.E.P., Jenkins, M.: Time Series Analysis: Forecasting and Control. Holden-Day, San Francisco (1976)

Bisaglia, L., Bordignon, S., Lisi, F.: k-Factor GARMA models for intraday volatility forecasting. Appl. Econom. Lett. **10**, 251–254 (2003)

Caporale, G.M., Gil-Alana, L.A.: Multi-factor Gegenbauer processes and European inflation rates. J. Econ. Integr. **26**(2), 386–409 (2011)

Caporale, G.M., Gil-Alana, L.A.: Long-run and cyclical dynamics in the US stock market. J. Forecast. **33**(2), 147–161 (2014)

Chung, C.-F.: Estimating a generalized long memory process. J. Econom. **73**(1), 237–59 (1996)

Chung, C.-F.: A generalized fractionally integrated autoregressive moving average process. J. Time Ser. Anal. **17**(2), 111–140 (1996)

Davydov, J.A.: The invariance principle for stationary processes. Theory Probab. Appl. **15**, 487–498 (1970)

Diongue, A.K., Ndongo, M.: The k-factor GARMA process with infinite variance innovations. Commun. Stat. Simul. Comput. **45**(2), 420–437 (2016)

Dissanayake, G.S., Peiris, M.S., Proietti, T.: State space modeling of Gegenbauer processes with long memory. Comput. Stat. Data Anal. **100**, 115–130 (2016)

Dissanayake, G.S., Peiris, M.S., Proietti, T.: Fractionally differenced Gegenbauer processes with long memory: a review. Stat. Sci. **33**(3), 413–426 (2018)

Espejo, R., Leonenko, N., Olenko, A., Ruiz-Medina, M.: On a class of minimum contrast estimators for Gegenbauer random fields. TEST **24**, 657–680 (2015)

Feng, Y.: An iterative plug-in algorithm for decomposing seasonal time series using the Berlin-method. J. Appl. Stat. **40**, 266–281 (2013)
Ferrara, L., Guégan, D.: Forecasting with k-factor Gegenbauer processes: theory and applications. J. Forecast. **20**(8), 581–601 (2001)
Gil-Alana, L.A., Aye, G.C., Gupta, R.: Trends and cycles in historical gold and silver prices. J. Int. Money Finance **58**, 98–109 (2015)
Giraitis, L., Leipus, R.: A generalized fractionally differencing approach in long-memory modeling. Lith. Math. J. **35**(1), 53–65 (1995)
Giraitis, L., Hidalgo, J., Robinson, P.M.: Gaussian estimation of parametric spectral density with unknown pole. Ann. Stat. **29**(4), 987–1023 (2001)
Gray, H.L., Zhang, N.F., Woodward, W.A.: Correction to on generalized fractional processes. J. Time Ser. Anal. **15**, 561–562 (1994)
Gray, H.L., Zhang, N.F., Woodward, W.A.: On generalized fractional processes. J. Time Ser. Anal. **10**, 233–257 (1989)
Grimmett, G., Stirzaker, S.: Probability Theory and Random Processes. Cambridge University Press, Cambridge (2020)
Hassler, U.: (Mis)specification of long memory in seasonal time series. J. Time Ser. Anal. **15**, 19–30 (1994)
Heiler, S., Feng, Y.: Data-driven decomposition of seasonal time series. J. Stat. Plan. Inference **91**, 351–363 (2000)
Hidalgo, J.: Semiparametric estimation for stationary processes whose spectra have an unknown pole. Ann. Stat. **33**, 1843–1889 (2005)
Hidalgo, J.: A nonparametric test for weak dependence against strong cycles and its bootstrap analogue. J. Time Ser. Anal. **28**(3), 307–349 (2007)
Hidalgo, J., Soulier, P.: Estimation of the location and exponent of the spectral singularity of a long memory process. J. Time Ser. Anal. **25**, 55–81 (2004)
Hosking, J.R.M.: Fractional differencing. Biometrika **68**(1), 165–176 (1981)
Hsu, N., Tsai, H.: Semiparametric estimation for seasonal long-memory time series using generalized exponential models. J. Stat. Plan. Inference **139**, 1992–2009 (2009)
Hunt, R., Peiris, S., Weber, N.: Estimation methods for stationary Gegenbauer processes. Stat. Pap. **63**, 1707–1741 (2022)
Janowiak, J.E.: An investigation of interannual rainfall variability in Africa. J. Clim. **1**, 240–255 (1988)
Kabitz, H.-J., Walterspacher, S., Walker, D., Windisch, W.: Inspiratory muscle strength in chronic obstructive pulmonary disease depending on disease severity. Clin. Sci. **113**(5), 243–249 (2007). https://doi.org/10.1042/CS20060362
Lapsa, P.: Determination of Gegenbauer-type random process models. Sig. Process. **63**, 73–90 (1997)
Leschinski, C., Sibbertsen, P.: Model order selection in periodic long memory models. Econom. Stat. **9**, 78–94 (2019)
Lustig, A., Charlot, P., Marimoutou, V.: The memory of ENSO revisited by a 2-factor Gegenbauer process. Int. J. Climatol. **37**, 2295–2303 (2017)
McElroy, T.S., Holan, S.H.: On the computation of autocovariances for generalized Gegenbauer processes. Stat. Sin. **22**, 1661–1687 (2012)
Montanari, A., Rosso, R., Taqqu, M.S.: A seasonal fractional ARIMA model applied to Nile river monthly flows at Aswan. Water Resour. Res. **36**, 1249–1259 (2000)
Olenko, A.: Limit theorems for weighted functionals of cyclical long-range dependent random fields. Stoch. Anal. Appl. **31**(2), 199–213 (2013)
Palma, W., Chan, N.H.: Efficient estimation of seasonal long-range-dependent processes. J. Time Ser. Anal. **26**, 863–892 (2005)
Pipiras, V., Taqqu, M.S.: Long-Range Dependence and Self-Similarity. Cambridge University Press, Cambridge (2017)
Porter-Hudak, S.: An application of the seasonal fractionally differenced model to the monetary aggregates. J. Am. Stat. Assoc. **85**, 338–344 (1990)
Ramachandran, R., Beaumont, P.: Robust estimation of GARMA model parameters with an application to cointegration among interest rates of industrialized countries. Comput. Econ. **17**(2/3), 179–201 (2001)
Ray, B.K.: Modeling long-memory processes for optimal long-range prediction. J. Time Ser. Anal. **14**, 511–525 (1993)

Regmi, B., Friedrich, J., Jörn, B., Senol, M., Giannoni, A., Boentert, M., Daher, A., Dreher, M., Spiesshofer, J.: Diaphragm muscle weakness might explain exertional dyspnea 15 months after hospitalization for COVID-19. Am. J. Respir. Crit. Care Med. (2023). https://doi.org/10.1164/rccm.202206-1243OC

Reisen, V.A., Zamprogno, B., Palma, W., Arteche, J.: A semiparametric approach to estimate two seasonal fractional parameters in the SARFIMA model. Math. Comput. Simul. **98**, 1–17 (2014)

Schuster, A.: On the investigation of hidden periodicities with application to a supposed 26 day period of meteorological phenomena. J. Geophys. Res. **3**(1), 13–41 (1898)

Spiesshofer, J., Kersten, A., Geppert, J.E., Regmi, B., Senol, M., Kabitz, H.-J., Dreher, M.: State-of-the-art opinion article on ventilator-induced diaphragm dysfunction: update on diagnosis, clinical course, and future treatment options. Respiration **102**(1), 74–82 (2023). https://doi.org/10.1159/000527466

Walterspacher, S., Pietsch, F., Walker, D.J., Röcker, K., Kabitz, H.-J.: Activation of respiratory muscle training. Respir. Physiol. Neurobiol. **247**, 126–132 (2018). https://doi.org/10.1016/j.resp.2017.10.004

Whitcher, B.: Wavelet-based estimation for seasonal long-memory processes. Technometrics **46**(2), 225–238 (2004)

Woodward, W.A., Cheng, Q.C., Gray, H.L.: A k-factor GARMA long-memory model. J. Time Ser. Anal. **19**(4), 485–504 (1998)